Azubuike and Sundararaj
Functional Composite Materials (2022) 3:3
https://doi.org/10.1186/s42252-022-00031-x

Functional Composite Materials

RESEARCH Open Access

Exploring the effect of block copolymer architecture and concentration on the microstructure, electrical conductivity and rheological properties of PP/PS blend nanocomposites

Lilian Azubuike and Uttandaraman Sundararaj*

Abstract

The interface between polymer matrices and nanofillers is critical for efficient interaction to achieve the desired final properties. In this work, block copolymers were utilized to control the interface and achieve optimum interfacial interaction. Specifically, we studied the compatibilizing effects of styrene-ethylene/butadiene-styrene (SEBS) and styrene-ethylene/propylene (SEP) block copolymers on the morphology, conductivity, and rheological properties of polypropylene-polystyrene (PP/PS) immiscible blend with 2 vol% multiwall carbon nanotube (MWCNT) at different blend compositions of PP/PS 80:20, 50:50 and 20:80.

MWCNTs induced co-continuity in PP/PS blends and did not obstruct with the copolymer migration to the interface. Copolymers at the interface led to blend morphology refinement. Adding block copolymers at a relatively low concentration of 1 vol% to compatibilize the PP/PS 80:20 blend substantially increased the electrical conductivity from $5.15*10^{-7}$S/cm for the uncompatibilized blend to $1.07*10^{-2}$S/cm for the system with SEP and $1.51*10^{-3}$S/m for the SEBS system. These values for the compatibilized blends are about 4 orders of magnitude higher due to the interconnection of the droplet domains. For the PP/PS 50:50 blend, the SEBS copolymer resulted in a huge increase in conductivity at above 3 vol% concentration (conductivity increased to $3.49*10^{-3}$S/cm from $5.16*10^{-7}$S/cm). Both the conductivity and the storage modulus increased as the SEBS copolymer content was increased. For the PP/PS 20:80 blend, we observed an initial decrease in conductivity at lower copolymer concentrations (1–3 vol%) and then an increase in conductivity to values higher than the uncompatibilized system, but only at a higher copolymer concentration of 10 vol%. The triblock copolymer (SEBS), which had 60 wt% PS content, shows a more significant increase in rheological properties compared to the diblock copolymer (SEP). The morphology shows that the interaction between MWCNT and PS is stronger than the interaction between MWCNT and PP, hence there is selective localization of the nanofiller in the PS phase as predicted by Young's equation and by molecular simulation.

Keywords: Compatibilization, Polypropylene, Polystyrene, SEBS, SEPs, Conductivity, Rheology, Polymer blend nanocomposite, Selective localization, Block copolymer, Carbon nanotube (CNT)

Introduction

The performance of the polymer blends greatly depends on the interfacial interaction and the interfacial tension of the constituent materials in the blend system and

*Correspondence: u.sundararaj@ucalgary.ca
Department of Chemical and Petroleum Engineering, University of Calgary, 2500 University Drive NW, Calgary, AB T2N 1N4, Canada

morphology [1, 2]. Good understanding of the interfacial communication will help in the design of composites to obtain excellent electrical and mechanical performance. Some applications of these materials include electromagnetic interference shielding such as those required in personal electronics, batteries, and electrostatic applications like electronics packaging [3–5].

Adding pre-made copolymers or creating copolymers via interfacial reaction are the major methods employed to enhance the phase compatibility in polymer blends [6, 7] and the copolymer changes the interface and blend rheology; and blend morphologies are affected by interfacial properties and rheological properties [8] of the blend components. The compatibilization mechanism is used to develop the mixing of the phases and to controlem the morphology of an immiscible polymer blend. Polymer blends are generally immiscible and this results most times in poor performance of the system due to the large domains of the dispersed phase and poor adhesion between the phases [9]. The most popularly used immiscible blends are compatibilized, and their final properties can be optimized by controlling the blend morphology [10]. Addition of nanofillers such as carbon nanotubes (CNTs), into immiscible blend systems results in a more complex system: polymer blend nanocomposites. In this system, polymer-polymer interaction, CNT-CNT interactions, and polymer-CNT interaction (see Fig. 1) are all important to determine the composites' final properties [12].

CNTs is the most popular one dimensional nanofiller used in polymers, due to its outstanding electrical conductivity, mechanical and thermal properties, and high aspect ratio [13]. High aspect ratio may assist either or both phases to wet CNTs and it is possible that CNT will locate at the interphase region between the two polymers, and this is good a strategy to tune the properties of the final product. The coexistence of CNT-polymer and CNT-CNT interactions helps in designing the structure and general properties of the polymer nanocomposites [11, 14]. Factors that affect these interactions include filler arrangement, network structure, polymer chain mobility, polymer molecular weight and most importantly the interphase performance. To enhance the adhesion among the different components in the polymer blend-CNT composites, a positive communication is required between the CNTs and the polymers to achieve some connection between the inorganic-organic interface, to increase electrical connectivity, have more efficient stress transfer, and enhance heat transfer [7, 8].

One way that has been shown to successfully promote this interaction between filler and polymer is use of compatibilizer. Compatibilizers are employed in the processing of immiscible polymer blend, either through addition compatibilization (adding premade copolymer) or by in situ compatibilization [9, 12]. Pre-made copolymers are made with different structural configurations, providing versatility for special target applications [15, 16]. These copolymers, which acts as polymeric interfacial agents [17] comprises of two or more repeat units and can be grouped based on the arrangement of the different units [18]. Consequently, we have four major categories of the copolymers: block, branched, random, and alternate copolymers; block copolymers are extensively used for compatibilizing polymer blends. Block copolymers originated with the "discovery of termination free anionic polymerization" [19] when blocks of polymer chains are connected together. These blocks are each made of chemically distinct repeat units [19] and are synthetized by polymerizing one polymer chain (polymer A) in tandem with another polymer chain (polymer B), and so on for additional blocks, so we can have diblock copolymers (two blocks), triblock copolymers (three blocks), and so on [20].

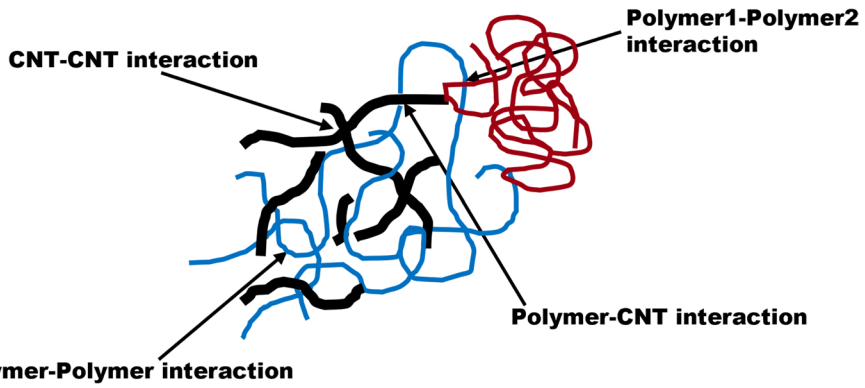

Fig. 1 Schematic illustration of polymer blend carbon nanotube interactions. Figure adapted from Ref [11]

Polymer blend compatibilization occurs at the interphase, for addition compatibilization the pre-made copolymers tends to locate at the interphase between the immiscible blends. This process results to steric stabilization of the droplet domain preventing coalescence, so we can achieve morphology refinement [10]. Bagheri-Kazemabad et al. [21] studied the relation between morphology and properties of polymer blends/clay nanocomposites. They found that in organo-modified nanoclay, when copolymers are added, they selectively locates in the phase with higher polarity in a PP/ethylene-octene copolymer/clay composite. Velankar et al. [22] mixed polyisobutylene (PIB) and polydimethylsiloxane (PDMS) compatibilized with several concentrations of diblock copolymer in 10:90 wt.% of PIB/PDMS blend composition. In their process, to allow for coalescence the shear rate was reduced from the initial rate of $4.8\,s^{-1}$ to $1.2\,s^{-1}$. They observed that the presence of copolymer into the blend increased the critical capillary number Ca_c when compared with the neat blend, which demonstrates that compatibilized droplet domains are more stable, and do not break up as easily as the uncompatibilized ones. The process of compatibilization was also shown by Bharati, A. et al. [23], where high molecular weight of the of the random or block copolymer of PS-PMMA results to increase in the electrical conductivity as it enhanced the continuity of the PαMSAN phase in which the nanofillers is localized. Moreover, phase separation in immiscible polymer blend was also used by Bharati, A. et al. [24] to interfacially segregate compatibilizer to make bi-continuous structures resulting to low percolation threshold of MWCNT.

Van Hemelrijck et al. [25] in their study with polyisoprene (PI)/PDMS copolymer, at 10/90 wt.% blend composition, the storage modulus against frequency plot showed an extra shoulder which indicates an extra relaxation mechanism. They also observed that, the relaxation mode is not easily noticeable when the copolymer content is increased, and non-linear regularization methods were used to confirm the presence of the two relaxation modes in the compatibilized blends. Furthermore, molecular simulation calculations using Hildebrand solubility parameters by Sundararaj and co-workers [26] showed that the block copolymer interacts better with the individual polymers, PP or PS than with MWCNT. This indicates that when copolymers migrate to the interphase, they do not envelop the nanofiller, allowing it to localize at the thermodynamically preferred phase. During in situ compatibilization, there is a complex chemical interaction that takes place at the interphase between the two polymers, and hence, a copolymer is formed directly at the interface comprising of segments of each of the polymers in the blend. In some cases, graft copolymers are formed, as shown by Azubuike and Sundararaj [27], at the interface during mixing, and the copolymer is pinned at the interface, trapping and strategically locating the MWCNTs to achieve better network connection and enhanced properties. As the copolymer is trapped at the interphase, morphology stability is achieved but the viscosity is increased, and therefore increased energy input will be required to process the material [16].

Block copolymers was also shown to reduce the interfacial tension, this work by Macaúbas, P.H.P et al. [28, 29] compared the morphology and the interfacial tension emulsion curve of PP/PS (90/10) at different SEBS and SBS copolymer concentration. They inferred that the concentration of the compatibilizer at the interfacial tension levels off is lower than the concentration in which the average radius of the droplet levels off.

The rheological properties and interfacial properties are the key parameters that determine the size of dispersed phase during melt processing [10]; hence, for improved phase adhesion and stabilization of the blend morphology, block copolymers should be introduced as compatibilizer, and this will also enhance the final properties of the multiphase polymer system [18, 20]. Moreover, it has been shown that phase adhesion provides significant improvement in the mechanical properties of immiscible polymer blends [30]. In this study, multiwall carbon nanotubes (MWCNT) were incorporated as the nanofiller and styrene ethylene/butadiene styrene (SEBS) triblock copolymer and styrene ethylene/propylene styrene (SEP(s)) diblock copolymer were added as compatibilizer at different concentrations. The electrical conductivity and the rheological properties were investigated at different blend compositions of PP/PS. This work showcases the different morphology evolution based on compatibilizer type, and how the copolymer impacts the MWCNT network connection. Forming a conductive nanofiller network leads to achieving good electrical conductivity and mechanical properties of the blend, and this structure and properties can be correlated to the rheological measurements in the linear viscoelastic region.

Experimental

Materials and methods

The polymers used in this study are polypropylene (PP) Lumicene® MR2001 from Total SA with MFI = 25 g/10 min and polystyrene (PS) Styron® 666D from Americas Styrenics LLC MFI = 8 g/10 min. Multiwalled carbon nanotubes (MWCNTs) Nanocyl™ NC 7000 were used as the nanofillers. SEBS A1535HU triblock copolymer (60 wt% styrene content) and SEP G1730VO diblock copolymer (22.5 wt.% styrene) were kindly provided by Kraton™ Corporation.

Polymer blend Nanocomposites preparation

The polymer blends with and without copolymers were mixed in the Alberta Polymer Asymmetric Mini-mixer (APAM) [31]. All blend components were dried in an oven at 70 °C under vacuum for 24 h prior to mixing. The mixing procedure consisted of simultaneously blending the neat PP and neat PS with the copolymer and MWCNT. After mixing, the blended composite was allowed to cool in air at room temperature. These blended samples were used for microscopic characterization. The processing conditions were kept constant, T = 220 °C and N = 200 rpm, for all the samples during the mixing process. Polymer blend ratios of 80:20, 50:50, and 20:80 PP// PS were prepared, with different copolymer concentrations of 1, 3, 5 and 10 vol% while the amount of MWCNT, 2 vol% was kept constant in all composites. After mixing, compression molding was performed for 10 min at 45 MPa pressure, and the molded samples were used for rheological analysis.

Material characterization

The MWCNT localization in the blend nanocomposite was determined using transmission electron microscopy (TEM). Thin sections of the samples were prepared using an Ultracut E (Reichert-Jung) equipped with an FC4D (Reichert-Jung) cryomicrotomy attachment. Blocks were trimmed first with a Cryotrim 45 (Diatome, Hatfield, PA) and then sectioned with a cryo diamond knife (Diatome, Hatfield, PA) at -60 °C to -80 °C. The trimmed sections were then picked up in 20% sucrose and transferred to a 200-mesh copper grid. The TEM images were then captured with a Gatan Orius CCD camera installed on a Philips – FEI (Thermo Fisher Scientific), Morgagni 268 model, operating at 80 kV.

The morphology of the composites was studied using scanning electron microscopy (SEM). Images were captured using a FEI XM30 SEM (FEI Hillsboro OR, USA) at 20 kV accelerating voltage. The samples were cryo-fractured in liquid nitrogen, and then etched using tetrahydrofuran (THF) to selectively remove the PS phase from all the blend composites. The etched surface was then sputtered with platinum before imaging to prevent sample degradation due to the electron beam.

The rheological measurements were performed using Anton-Paar MCR 302 rheometer at 220 °C, using 25 mm diameter parallel-plate geometry with gap size of 0.5 mm. All experiments were carried out at a temperature of 220 °C. Strain amplitude sweep was done on all the systems to demonstrate the linear viscoelastic regime (LVR). This test was performed over a range of applied strain amplitudes from 0.1% to 1000% at constant angular frequency of 1 rad/s. Subsequently, frequency sweep experiments at constant strain amplitude of 0.1% were done on the samples to investigate the structural evolution of the multiphase polymer blend nanocomposites, and to determine the extent of 3D network formation.

The DC electrical conductivity of all the complex blend systems was measured using a Loresta GP resistivity meter (MCP – T610 model Mitsubishi Chemical Co., Tokyo, Japan), connected to a four pin ESP probe (MCP, TP08P Model, Mitsubishi Chemical Co.). The measurement was carried out at an applied voltage of 90 V on three different samples for each blend system, the result reported is the average for each system.

Results and discussion

MWCNT localization and morphology

The TEM micrographs, presented in Fig. 2 shows the localization of MWCNT in the PP/PS 80:20 immiscible blends with 5 vol% copolymer and without the copolymers. We observed a significant amount of MWCNTs in the droplet phase (PS) in the absence of copolymers (see Fig. 2a_1). Introducing SEBS triblock copolymer did not affect the localization of the nanofillers in the system as seen in Fig. 2b, but for the diblock (SEPs) we observed some of the fillers at the interphase and in the matrix (PP) in Fig. 2c. This could be the result of some of the copolymers forming micelles during the melt mixing process and these micelles tended to migrate to the interphase. Subsequently, the nanofillers migration governed by shear induced collision [32] due to the shear generated during processing can result to its localization in the matrix. In addition, for the composite with the diblock copolymer, we also see localization of the nanofillers in the minor phase and some at the interface bridging two minor phases as shown in Fig. 2c_1. Pötschke et al. [33] and Nuzzo et al. [34] attributed the bridge to the small phase size of the encapsulating domain compared to the length of MWCNT but this is not the case in our system. Since MWCNT is in the preferred phase, the bridging is less a result of migration but more of the large size of the dispersed phase, resulting in clustering of the dispersed domains and subsequently resulting to interfacial deformation and bridging of MWCNT [35]. The localization of MWCNT at the interphase can be said to be because of the assembly of copolymer chains, which involves copolymer chain movement that might affect the MWCNT migration between the phases.

Scanning electron microscope (SEM) images were captured to study the different morphological structures developed by the different blend compositions and are shown in Fig. 3 and Fig. 4. SEM confirms that the block copolymers significantly influence the domain sizes. The large droplet size formed in the system without any copolymer can be seen to deform with addition of MWCNT. The interfacial deformation of the droplet

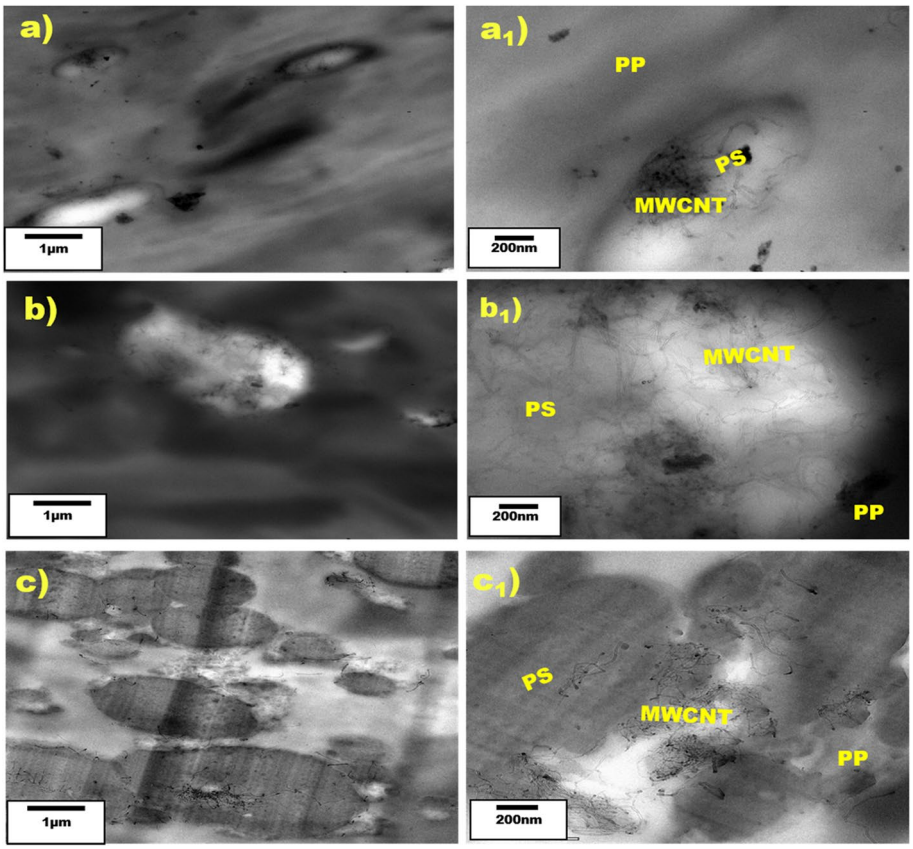

Fig. 2 TEM Images of 2 vol% MWCNT and 5 vol% copolymer a-a_1) PP/PS 80:20 b-b_1) PP/PS 80:20/SEBS-A1535 HU, c-c_1) PP/PS 80:20/SEPs- G1730VO

morphology can be attributed to nanofiller migration causing coalescence and elongation of the droplet domain [26]. Notably, the addition of triblock copolymers (Fig. 3) resulted in significant interconnection of the droplet domain at low copolymer concentration of 1 vol%. Upon increasing copolymer concentration to 3 vol% for the PP/PS 80:20 blend composition, the PS domain size decreases. Increasing the triblock copolymer in the 50:50 blend composition, we achieved a co-continuous morphology. The triblock has a higher styrene content of 60 wt% in the copolymer and thus, copolymer and MWCNT selectively localized in the PS phases. For the PP/PS 20:80 blend, the PP minor phase forms spherical droplets for all block copolymer concentrations, and there is a very significant effect on morphology at higher copolymer concentrations. These results show that the block copolymer controls the morphology development of the nanocomposite by halting the coalescence processes, especially in the 80:20 blend composition. Copolymers can suppress coalescence by steric stabilization of the interphase [6, 28] and/or Marangoni stresses [26, 28, 36–39].

It should be noted that at higher concentrations of block copolymer, it might act less like a compatibilizer between the two main phases (PP and PS) and rather like a third phase. In this work, our main purpose was to use the block copolymer as a compatibilizer, but we went up to 10 vol% copolymer to see the effect of concentration. We see from the SEM images in Figs. 3 and 4, that the compatiblization of the interface saturates at 1–3% copolymer concentration.

The block configuration (i.e. diblock or triblock) and the PS content in each copolymer influenced the morphology evolution in each blend system. For the PP/PS 80:20 system without copolymer, shown in Fig. 3a, we observe deformation of PS domains because of coalescence of the droplets. However, upon adding triblock copolymer, the coalescence is reduced for the 80:20 blend composition, though morphology is slightly co-continuous. Because a significant amount of nanofillers locate in PS domain, and the block copolymer locates at the interface with the styrene segments of the triblock copolymer inside the PS droplet and the ethylene/butadiene segment in the PP matrix, droplet coalescence is suppressed

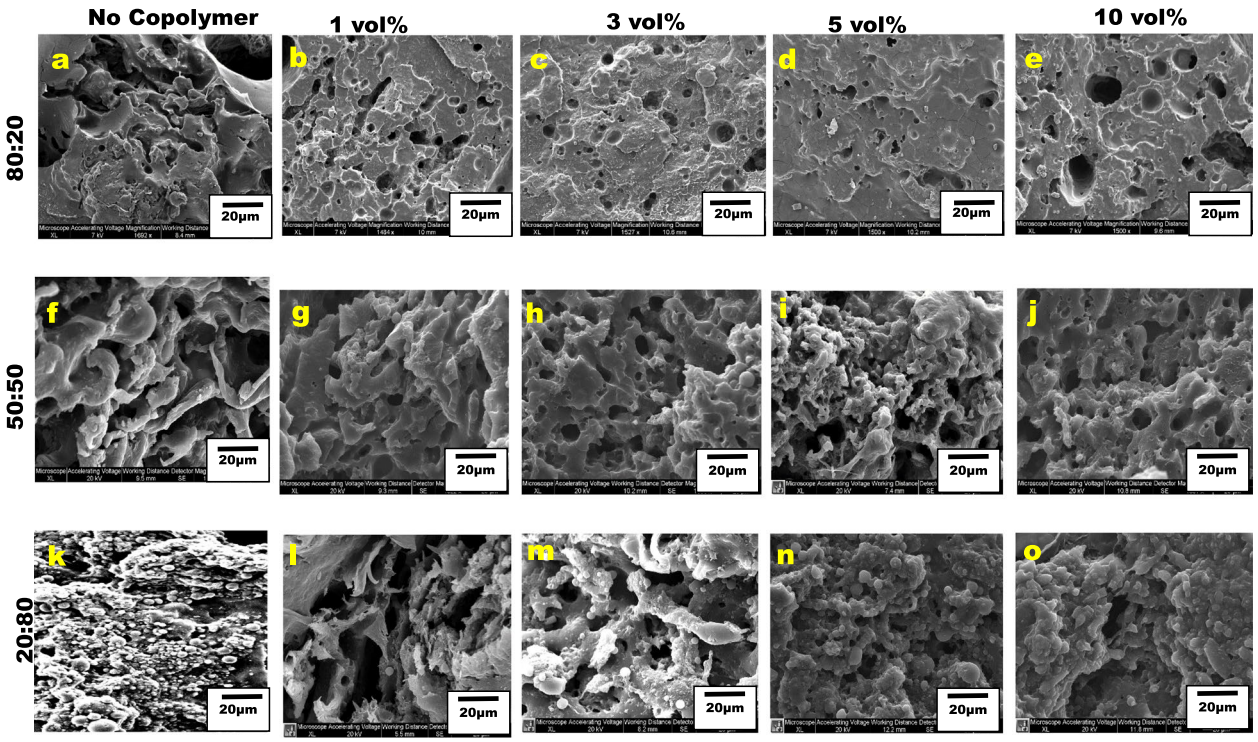

Fig. 3 SEM micrographs of PP/PS/ 2 vol% MWCNT/ SEBS triblock copolymer. From left to right, the triblock copolymer concentration increases and from top to bottom, PS amount increases in the blend composition. PS phase was extracted in all the composites using THF

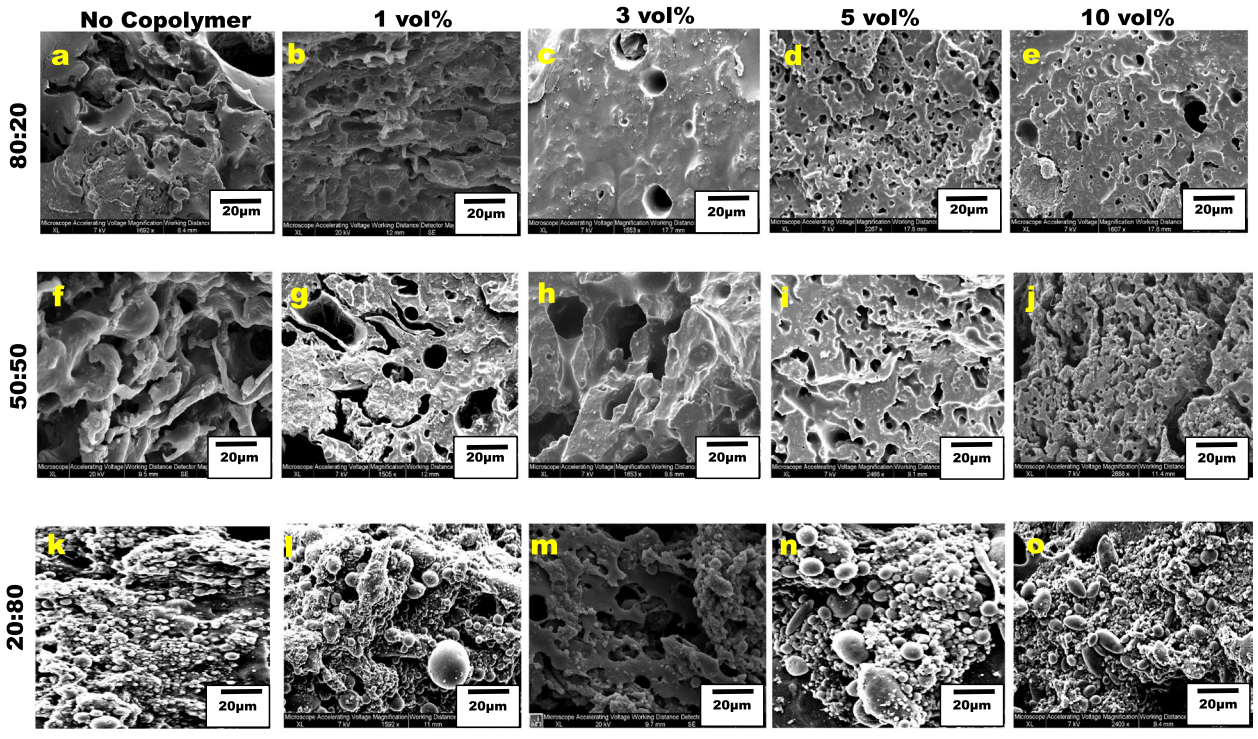

Fig. 4 SEM Micrograph of PP/PS/ 2 vol% MWCNT/ SEP diblock copolymer. Going from left to right, the diblock copolymer concentration increases and going from top to bottom PS amount increases in the blend composition PS phase was extracted in all the composites using THF

as the copolymer content increases. That is, the copolymer forms a barrier layer at the interphase and does not allow the PS molecules in adjacent droplets to interact and the MWCNT in the droplets increases the viscosity of the droplet phase not allowing PS to flow as easily.

At higher PS content in 50:50 blend, there is more interfacial area and the MWCNT content in PS phase is lower (though it is the same in the overall blend composition) and with triblock copolymer, the droplets tend to connect slightly as shown in Fig. 3(g-j). However, this is not the case when we add diblock copolymer (Fig. 4(g-j)), and we observe a reduced droplet domain size. This may be due to the lower PS content of the copolymer inside the PS droplet, keeping the copolymer at the interphase. The PS/MWCNT domain also significantly reduced, and the droplet shapes are more irregular and do not form a continuous phase like in the case of the blend with triblock copolymer. Increasing PS concentration to 80% in the 20:80 PP/PS blend system shows similar morphology evolution for diblock copolymer as that observed for the triblock.

Rheology

Some previous research has shown that addition of compatibilizers on the blend greatly affects the blend morphology during mixing [6, 29, 31] and the morphology in turn affects the blend rheology. We studied the rheology of the blend components and viscosity ratio (η_d/η_m) at the processing condition and was calculated as 3.28 as shown in Fig. S1, this high viscosity ratio contributed to the interfacial deformation observed in Fig. 3a and 4a. In addition, the linear rheological tests of the polymer blend nanocomposite were conducted to study the effect of copolymers on the morphology of the immiscible blend systems. Fig. 5 shows the frequency and strain amplitude sweeps of different PP/PS/SEBS blend compositions, with 2 vol% MWCNT., In PP/PS 80:20 polymer blend nanocomposites (Fig. 5a, b), at 1 vol% concentration of the SEBS copolymer, we achieved about two orders of magnitude increase compared to the uncompatibilized blend nanocomposite and a corresponding plateau-like behavior in the low-frequency region. This can be explained by the interconnection of the droplet domains shown in Fig. 3b, and the formation of a 3-dimensional network structure of MWCNT [40]. Introducing SEBS block copolymer resulted in a significant increase in the storage modulus for the PP/PS 50:50 and 20:80 blend compositions shown in Fig. 5c-f, and generally, there is a increase in modulus with increasing copolymer content; hence, there is an associated increase in the stiffness of the nanocomposites. This can be linked to the formation of a 3-dimensional network structure of MWCNT with addition of SEBS and to the high elasticity of SEBS copolymer as shown in Fig. S2. In addition, this increase can also be partly attributed to the transformation of the morphology from dispersed to co-continuous morphology induced by MWCNT localized in the PS phase [41], as seen from the SEM micrographs, Fig. 3(g-j). This can also explain the droplet size reduction and the corresponding increase of interfacial area in the PP/PS 80:20 blend nanocomposite. These changes are attributed to the increase in interfacial elasticity [32, 33] due to MWCNT and consequently, we see stabilization in the morphology. For the PP/PS 80:20 blend nanocomposite, we see the highest storage modulus for 1 vol% SEBS (Fig. 5a) and subsequently a drop in modulus at 3 vol% SEBS, we see the finest droplet morphology for this nanocomposite (Fig. 3c). Moreover, for the PP/PS 50:50 and 20:80 blend nanocomposites, the observed co-continuous morphology with additional SEBS copolymer contributed to the increase in storage modulus and loss modulus behavior shown in Fig. S3 of the blend system. Although the SEP diblock copolymer gives a more regular and reduced droplet size, and higher interfacial area, the SEBS triblock resulted in the highest moduli and impacted the linear viscoelastic properties more because of a more connected network due to SEBS having a higher PS content.

Figure 6 shows the frequency and strain amplitude of the storage modulus for the different blend compositions and copolymer concentrations for blend nanocomposites made with SEP diblock copolymer. In general, we observed that higher concentration of 10 vol% of diblock copolymer, gave higher modulus at low strain and same also applies for the loss modulus in Fig. S4, and a lower critical strain amplitude compared to the other diblock concentrations. This can be attributed to the interconnected PS-CNT domains, since at high copolymer concentration, there are more interconnections at the interface as the copolymer bridges the two phases [42, 43]. The combined effect of MWCNT and copolymer in PS is to stretch the PS.

Domains until they link with each other. Consequently, we achieved a more connected network structure. To understand the individual effects of the copolymer on the blend system without CNTs, we carried out a strain sweep of the blend systems with 5 vol% of copolymers, shown in Fig. S5. In both cases, the increase in moduli is less without the MWCNT. However, a very significant increase in modulus and a low critical strain amplitude was observed for SEBS triblock (60 wt% PS), and this corresponded with the increased moduli observed for the PP/PS/SEBS/MWCNT blend nanocomposite systems compared to those made with SEP.

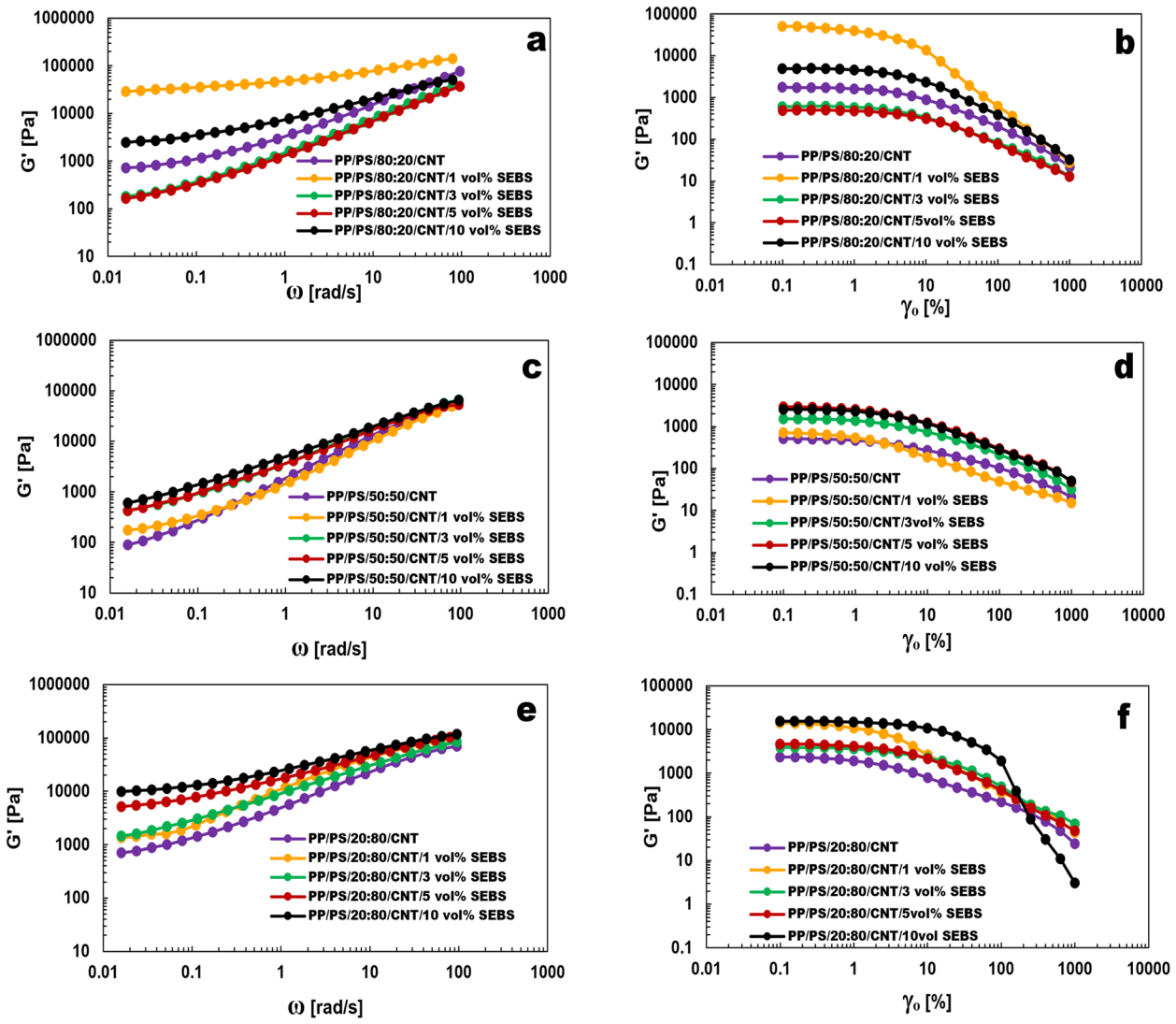

Fig. 5 Frequency and strain sweep of PP/PS/MWCNT/SEBS triblock at different concentration **a-b**) 80:20, **c-d**) 50:50, and **e-f**) 20:80 blend compositions

Electrical conductivity

The DC conductivity for different blend nanocomposite systems with different block copolymers, at different blend compositions of the PP/PS, were measured and plotted against the copolymer concentrations, and the plots are shown in Fig. 7. The PS/CNT single polymer nanocomposite shows a very high conductivity (just over 10^{-2} S/cm) compared to the very low conductivity of PP/CNT (just below 10^{-6} S/cm) in the absence of any compatibilizer. This result indicates that CNT has better affinity for PS and agrees with the molecular simulation done by Sundararaj and co-workers [26], which showed that PS has higher binding energy for CNT and hence will have a much better interaction. This higher binding energy between CNT and PS can be correlated to better dispersion and distribution of CNT in the PS matrix, resulting in high conductivity, and in selective localization of CNT in PS phase for PP/PS blends, although subsequent increase in copolymer concentration in the single polymer nanocomposite increases the conductivity as shown in Fig. S6.

Introducing block copolymers to PP/PS 80:20 blend nanocomposites, we obtained a high conductivity at 1 vol% copolymer concentration for both copolymers. At this concentration, the PS/MWCNT domain interconnectivity is enhanced, as shown in the SEM micrographs in Fig. 3b and Fig. 4b, and as shown by the increased rheology at 1 vol% copolymer

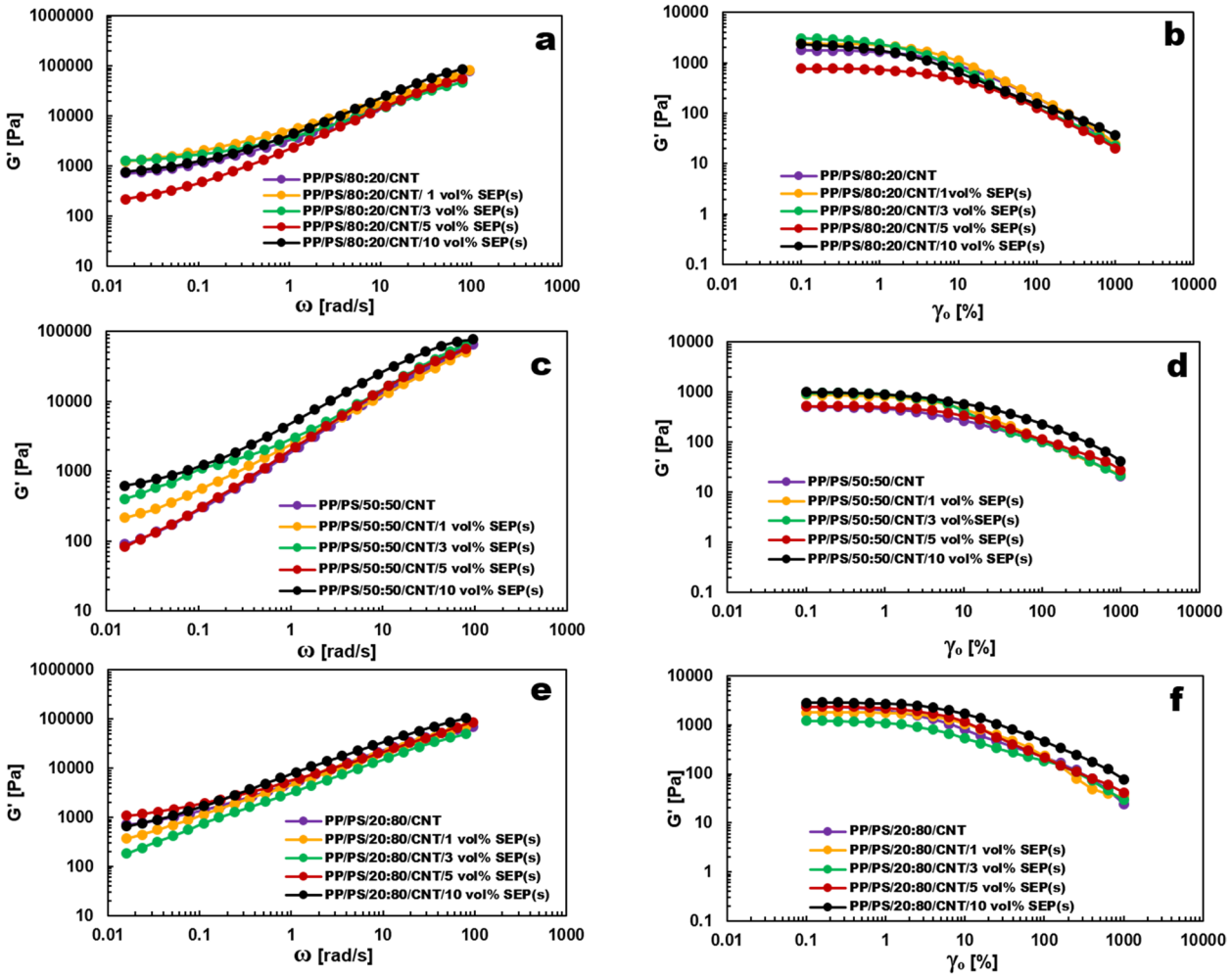

Fig. 6 Frequency and strain sweep of PP/PS/MWCNT/SEP(s) diblock at different concentration **a-b**) 80:20, **c-d**) 50:50, and **e-f**) 20:80 blend compositions

in Fig. 5a and Fig. 6a. This better PS/MWCNT domain interconnectivity in the PP/PS 80:20 blend system led to the significant increase in conductivity (four orders of magnitude increase) over PP/MWCNT nanocomposite, as seen in Fig. 7a. Increasing the copolymer concentration at this same blend composition results in substantial reduction of the PS domain interconnectivity due to the stabilization of the droplet morphology by the copolymer, i.e. high concentration of copolymer suppresses droplet coalescence and domain interconnectivity seen for 1 vol%. Since MWCNT selectively locates in PS, reduced PS interconnectivity results in a disruption of the CNT network, and hence, we see a very large drop in the conductivity of the blend system as the copolymer concentration increases beyond 1 vol%, and the conductivity is similar to the uncompatibilized PP/PS 80:20 system.

For the PP/PS 50:50 blend nanocomposite, we observed the opposite result upon adding copolymers, with a dramatic increase in conductivity at 3 vol% copolymer concentration for the system with the triblock copolymer. At higher concentrations (10 vol% copolymer), both the triblock and diblock systems show higher conductivity (three orders of magnitude increase). This agrees with the co-continuous morphology observed in the microstructure, shown in Fig. 3j and Fig. 4j and also in the frequency sweep and strain sweep results in Fig. 5c-d and 6c-d, respectively, where we obtained a high storage modulus at higher copolymer concentration, indicating that we had established a 3D network structure. This trend in conductivity increase for the SEBS triblock copolymer system is not seen in the system with SEP(s) diblock copolymer, except at 10 vol% SEP, where a significant increase in conductivity about 3 orders of magnitude was observed in agreement with the high modulus

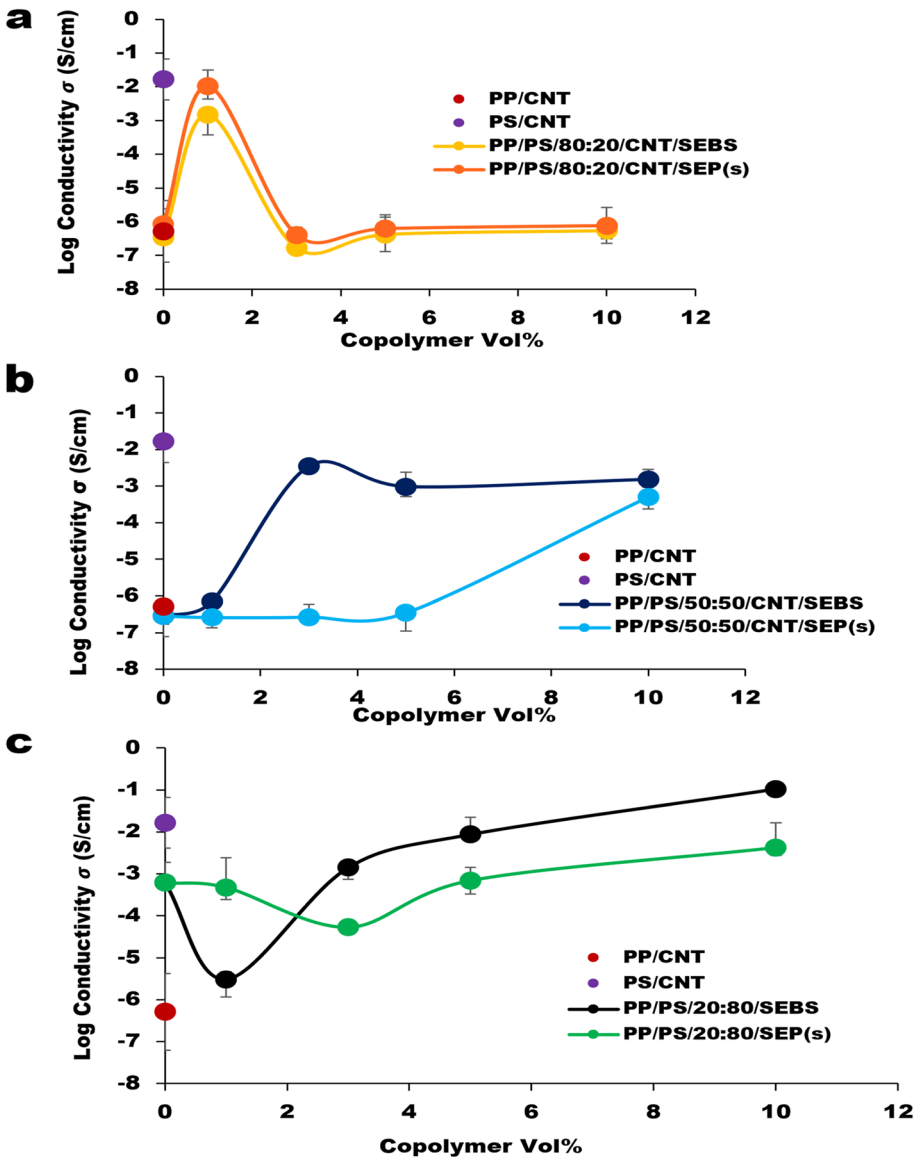

Fig. 7 Electrical conductivity, **a**) PP/PS 80:20 **b**) PP/PS 50:50 **c**) PP/PS 20:80, with 2 vol% MWCNT at different copolymer concentrations. Adding copolymer to the blend nanocomposite system has enormously different electrical conductivity trends based on copolymer type and concentration

in the rheological result. The co-continuous morphology obtained (Fig. 4j) can be attributed to the chain assembly of the copolymer at high concentration.

In PP/PS 20:80 blend composition, we see a drop in the conductivity at low copolymer concentrations. For the PP/PS 20:80 system, as the copolymer goes into the polymer blend and to the interphase, it may break up the MWCNT structure built inside the matrix PS phase. As the quality of the CNT domain connection decreases, we obtain lower conductivity, but at higher copolymer concentration, may form a more connected structure and create a more co-continuous structure in the blend. In the system with triblock copolymer, at 1 vol% SEBS, the MWCNT network is disrupted, and we see a huge drop in electrical conductivity (from $6.17*10^{-4}$S/cm to $3.07*10^{-6}$S/cm). At higher SEBS concentrations, the conductivity increases, with a value of $1.05*10^{-1}$S/cm at 10 vol% SEBS. Considering the high PS concentration of SEBS copolymers, there can be a significant co-continuous PS block phase and MWCNT network, leading to an increase in conductivity over the uncompatibilized blend. Moreover, there is a significant drop in

conductivity at 3 vol% for SEP diblock copolymer also as shown in Fig. 7c, and this drop in conductivity matches with reduced modulus as shown in Fig. 6e, signifying a poor MWCNT network connection.

Conclusion

In this study, we examined the impact of different block copolymer architecture on immiscible polymer blend nanocomposites with 2 vol% MWCNT at different polymer blend and copolymer compositions. Using different copolymer structures and concentration, we obtained different morphological structures, which were correlated to the rheological and electrical properties of the polymer blend nanocomposites (PP/PS/2 vol% MWCNT). Using 1% concentration of either diblock SEP or triblock SEBS, we achieved better PS/MWCNT domain interconnectivity in the PP/PS 80:20 blend system that led to a significant increase in conductivity (four orders of magnitude increase). The increased conductivity corresponded to an increase in storage modulus at 1% copolymer content. Interestingly, the conductivity and rheology results decreased at higher copolymer contents up to 10% in the PP/PS 80:20 blend system.

A substantially different morphology evolution is observed in the PP/PS 50:50 blend composition. Here, adding triblock copolymer to the blend nanocomposite results in a more co-continuous morphology compared to that obtained by adding the diblock copolymer. This difference in morphology changed the electrical conductivity of the system and we achieved 4 orders of magnitude increase in electrical conductivity with 3% triblock SEBS copolymer, and the conductivity remained high up to 10%. Only at high diblock SEP copolymer concentration (10%) were we able to achieve a significant 4 orders of magnitude increase in conductivity in the PP/PS 50:50 system, and we attributed this to the copolymer chain assembly at the interface. The rheological parameters, namely the storage modulus, matched the electrical results, showing a rheological percolation at 1 vol% SEBS and then a decrease in modulus at higher copolymer concentrations. In the PP/PS 20:80 system, we saw an initial decrease in the electrical conductivity at low copolymer concentrations (1 vol%) but subsequently, at 10 vol% SEBS, the conductivity increased by two orders of magnitude over that of the uncompatibilized blend nanocomposite, presumably due to the formation of a co-continuous PS block phase in which there was a MWCNT network.

The viscoelastic properties of the blend nanocomposites of our system were influenced by the addition of the triblock SEBS copolymer, and we achieved a greater increase in storage modulus at all blend compositions with SEBS, compared to SEP. This was linked to several factors including the high PS content in the SEBS copolymer, MWCNT localizing in the PS domain, and migration of CNT (especially for PP/PS 50:50 and PP/PS 20:80) resulting in a co-continuous morphology. In summary, we observed different morphological evolutions by varying concentrations of the block copolymers, with the triblock copolymer showing a more significant impact on the conductivity and rheological parameters, especially at the 50:50 and 20:80 PP/PS blend composition.

Supplementary Information

The online version contains supplementary material available at https://doi.org/10.1186/s42252-022-00031-x.

Additional file 1.

Acknowledgments

We would like to acknowledge the financial support of Natural Sciences and Engineering Research Council of Canada (NSERC) Discovery Grant DG-05503-2020 and Canada Foundation for Innovation Leaders Opportunity Fund (LOF). We would also like to thank Dr. Ivonne Otero-Navas for her kind contributions to the planning of experiments and reviewing of the manuscript. We would like to also thank Petroleum Technology Development Fund (PTDF).

Authors' contributions

Lilian Azubuike: Conceptualization, methodology, formal analysis, investigation, data curation, writing original draft preparation, review, editing, and visualization. Uttandaraman Sundararaj: Conceptualization, formal analysis, writing, review and editing, visualization, supervision, funding acquisition. The authors read and agreed to the published version of the manuscript.

Funding

This research was supported by the Natural Sciences and Engineering Research Council of Canada (NSERC).

Availability of data and materials

The data presented in this study are available on request from the corresponding author.

Declarations

Competing interests

The authors declare no conflict of interest.

Received: 26 December 2021 Accepted: 28 March 2022
Published online: 12 April 2022

References

1. J.S. Higgins, Polymer blends. Makromol. Chem. Macromol. Symp. **15**(1), 201–213 (1988)
2. M. Entezam, H. Poormadadkar, H.A. Khonakdar, S.H. Jafari, Melt rheology and interfacial properties of binary and ternary blends of PS, EOC, and SEBS. J. Appl. Polym. Sci. **48791**, 1–13 (2019)
3. M.H. Al-Saleh, U. Sundararaj, Nanostructured carbon black filled polypropylene/polystyrene blends containing styrene-butadiene-styrene copolymer: Influence of morphology on electrical resistivity. Eur. Polym. J. **44**(7), 1931–1939 (2008)
4. J.C. Huang, Carbon black filled conducting polymers and polymer blends. Adv. Polym. Technol. **21**(4), 299–313 (2002)
5. D.D.L. Chung, Electromagnetic interference shielding effectiveness of carbon materials. Carbon N. Y. **39**(2), 279–285 (2001)

6. X. Qi et al., Selective localization of carbon nanotubes and its effect on the structure and properties of polymer blends. Prog. Polym. Sci. **123**, 101471 (2021)
7. C. Xu, Y. Tan, Y. Song, Q. Zheng, Influences of compatibilization and compounding process on electrical conduction and thermal stabilities of carbon black-filled immiscible polypropylene/polystyrene blends. Polym. Int. **62**(2), 238–245 (2013)
8. A. Ajji, L.A. Utracki, Interphase and compatibilization of polymer blends. Polym. Eng. Sci. **36**(12), 1574–1585 (1996)
9. L.A. Utracki, C.A. Wilkie, *Polymer blends handbook* (2014)
10. U. Sundararaj, C.W. Macosko, Drop breakup and coalescence in polymer blends: the effects of concentration and compatibilization. Macromolecules. **28**(8), 2647–2657 (1995)
11. I. Alig et al., Establishment, morphology and properties of carbon nanotube networks in polymer melts. Polymer (Guildf). **53**(1), 4–28 (2012)
12. J. Parameswaranpillai et al., Tailoring of interface of polypropylene/polystyrene/carbon nanofibre composites by polystyrene-block-poly (ethylene-ran-butylene)-block-polystyrene. Polym. Test. **51**, 131–141 (2016)
13. M. Bhattacharya, Polymer nanocomposites-a comparison between carbon nanotubes, graphene, and clay as nanofillers. Materials (Basel). **9**(4), 1–35 (2016)
14. T. Drwenski, S. Dussi, M. Dijkstra, R. Van Roij, P. Van Der Schoot, Connectedness percolation of hard deformed rods. J. Chem. Phys. **147**(22), 224904 (2017)
15. M. Xanthos, S.S. Dagli, Compatibilization of polymer blends by reactive processing. Polym. Eng. Sci. **31**(13), 929–935 (1991)
16. L.A. Utracki, Compatibilization of polymer blends. Can. J. Chem. Eng. **80**(6), 1008–1016 (2002)
17. G. Radonjic, "Compatibilization effects of styrenic / rubber Block bopolymers in polypropylene / polystyrene blends". J. Appl. Polym. Sci. **72**, 291–307 (1999)
18. J. Lewis, Introduction to polymer capacitors. Electron. Prod. **55**(11) (2013). https://www.electronicproducts.com/Passive_Components/Capacitors/Introduction_to_polymer_capacitors.aspx.
19. F.S. Bates, G.H. Fredrickson, Block copolymer thermodynamics: theory and experiment. Annu. Rev. Phys. Chem. **41**(1), 525–557 (1990)
20. N. Hadjichristidis, S. Pispas and G. Floudas. *Block Copolymers: Synthetic Strategies, Physical Properties, and Applications* (Wiley, 2003)
21. S. Bagheri-Kazemabad et al., Morphology, rheology and mechanical properties of polypropylene/ethylene-octene copolymer/clay nanocomposites: Effects of the compatibilizer. Compos. Sci. Technol. **72**(14), 1697–1704 (2012)
22. S. Velankar, P. Van Puyvelde, J. Mewis, P. Moldenaers, Effect of compatibilization on the breakup of polymeric drops in shear flow. J. Rheol. (N. Y. N. Y). **45**(4), 1007–1019 (2001)
23. A. Bharati, R. Cardinaels, T. Van der Donck, J.W. Seo, M. Wübbenhorst, P. Moldenaers, Tuning the phase separated morphology and resulting electrical conductivity of carbon nanotube filled PαMSAN/PMMA blends by compatibilization with a random or block copolymer. Polymer. (Guildf). **108**, 483–492 (2017)
24. A. Bharati, R. Cardinaels, J.W. Seo, M. Wübbenhorst, P. Moldenaers, Enhancing the conductivity of carbon nanotube filled blends by tuning their phase separated morphology with a copolymer. Polymer. (Guildf). **79**, 271–282 (2015)
25. E. Van Hemelrijck, P. Van Puyvelde, S. Velankar, C.W. Macosko, P. Moldenaers, Interfacial elasticity and coalescence suppression in compatibilized polymer blends. J. Rheol. (N. Y. N. Y). **48**(1), 143–158 (2004)
26. I.O. Navas, M. Kamkar, M. Arjmand, U. Sundararaj, Morphology evolution, molecular simulation, electrical properties, and rheology of carbon nanotube/polypropylene/polystyrene blend nanocomposites: effect of molecular interaction between styrene-butadiene block copolymer and carbon nanotube. Polymers (Basel). **13**(2), 1–25 (2021)
27. L. Azubuike, U. Sundararaj, Interface strengthening of ps/apa polymer blend nanocomposites via in situ compatibilization: enhancement of electrical and rheological properties. Materials (Basel). **14**(17), 4813 (2021). https://doi.org/10.3390/ma14174813.
28. P.H.P. Macaúbas, N.R. Demarquette, Morphologies and interfacial tensions of immiscible polypropylene/polystyrene blends modified with triblock copolymers. Polymer (Guildf). **42**(6), 2543–2554 (2001)
29. I.M.O. Navas, *No Title* (2017)
30. V. Musil, S. Ivan, *Compatibilization of Polypropylene / Polystyrene Blends with Poly (styrene-b-butadiene-b-styrene) Block Copolymer* (2000), pp. 2625–2639
31. O. Breuer, U. Sundararaj, Big returns from small fibers: a review of polymer/carbon nanotube composites. Polym. Compos. **25**(6), 630–645 (2004)
32. J. Yang, X. Qi, N. Zhang, T. Huang, Y. Wang, Carbon nanotubes toughened immiscible polymer blends. Compos. Commun. **7**(October 2017), 51–64 (2018)
33. P. Pötschke, A.R. Bhattacharyya, A. Janke, Morphology and electrical resistivity of melt mixed blends of polyethylene and carbon nanotube filled polycarbonate. Polymer (Guildf). **44**(26), 8061–8069 (2003)
34. A. Nuzzo, E. Bilotti, T. Peijs, D. Acierno, G. Filippone, Nanoparticle-induced co-continuity in immiscible polymer blends - a comparative study on bio-based PLA-PA11 blends filled with organoclay, sepiolite, and carbon nanotubes. Polymer (Guildf). **55**(19), 4908–4919 (2014)
35. E.J. Dil, M. Arjmand, I.O. Navas, U. Sundararaj, B.D. Favis, Interface bridging of multiwalled carbon nanotubes in polylactic acid/poly (butylene adipate-co-terephthalate): morphology, rheology, and electrical conductivity. Macromolecules. **53**(22), 10267–10277 (2020)
36. S.P. Lyu, T.D. Jones, F.S. Bates, C.W. Macosko, Role of block copolymers on suppression of droplet coalescence. Macromolecules. **35**(20), 7845–7855 (2002)
37. E. Nowak, N.M. Kovalchuk, Z. Che, M.J.H. Simmons, Effect of surfactant concentration and viscosity of outer phase during the coalescence of a surfactant-laden drop with a surfactant-free drop. Colloids Surfaces A Physicochem. Eng. Asp. **505**, 124–131 (2016)
38. V. Cristini, Near-contact motion of surfactant-covered spherical drops: ionic surfactant. J. Colloid Interface Sci. **211**(2), 355–366 (1999)
39. P.G. Ghodgaonkar, U. Sundararaj, Prediction of dispersed phase drop diameter in polymer blends: The effect of elasticity. Polym. Eng. Sci. **36**(12), 1656–1665 (1996)
40. S.M.N. Sultana, S.P. Pawar, M. Kamkar, U. Sundararaj, Tailoring MWCNT dispersion, blend morphology and EMI shielding Properties by sequential mixing strategy in immiscible PS/PVDF blends. J. Electron. Mater. **49**(3), 1588–1600 (2020)
41. I. Otero-Navas, M. Arjmand, U. Sundararaj, Carbon nanotube induced double percolation in polymer blends: Morphology, rheology and broadband dielectric properties. Polymer (Guildf). **114**, 122–134 (2017)
42. C.R. López-Barrón, A.H. Tsou, Strain hardening of polyethylene/polypropylene blends via interfacial reinforcement with poly (ethylene-cb-propylene) comb block copolymers. Macromolecules. **50**(7), 2986–2995 (2017)
43. R. Salehiyan, H.Y. Song, M. Kim, W.J. Choi, K. Hyun, Morphological evaluation of PP/PS blends filled with different types of clays by nonlinear rheological analysis. Macromolecules. **49**(8), 3148–3160 (2016)

Publisher's Note